

# The Effect of Hall Current on Unsteady MHD Free Convective Couette Flow of a Bingham Fluid with Thermal Radiation

S. Harisingh Naik, K. Rama Rao, M. V. Ramana Murthy

**Abstract-** The objective of this study to find the numerical solution of unsteady magneto hydrodynamic flow of an electrically conducting viscous incompressible non – Newtonian Bingham fluid bounded by two parallel non – conducting porous plates is studied with thermal radiation considering the Hall Effect. An external uniform magnetic field is applied perpendicular to the plates and the fluid motion is subjected to a uniform suction and injection. The lower plate is stationary and the upper plate moves with a constant velocity and the two plates are kept at different but constant temperatures. The fluid is considered to be a gray, absorbing emitting but non – scattering medium and the Roseland approximation is used to describe the radioactive heat flux in the energy equation. Numerical solutions are obtained for the governing momentum and energy equations taking the Joule and viscous dissipations into consideration. The dimensionless governing coupled, non – linear boundary layer partial differential equations are solved by an efficient, accurate, and extensively validated and unconditionally stable finite difference scheme of the Crank – Nicolson method. The effects of the Hall term, the parameter describing the non – Newtonian behavior, thermal radiation parameter and the velocity of suction and injection on both the velocity and temperature distributions are studied through graphs and tabular form.

**Keywords:** Couette flow, Thermal radiation, Bingham fluid, Hall Effect and Finite difference method.

## I. INTRODUCTION

The fluid flow between parallel plates by means of Couette motion is a classical fluid mechanics problem that has applications in magneto hydrodynamic (MHD) power generators and pumps, accelerators, aerodynamics heating, electrostatic precipitation, polymer technology, petroleum industry, purification of crude oil, and also in many material processing applications such as extrusion, metal forming, continuous casting, wire and glass fiber drawing, etc. This problem has received considerable attention in the case of horizontal parallel plates [1] – [8] than vertical parallel plates. An analysis of flow formation in Couette motion between vertical parallel plates was presented by Schlichting and Gersten [9]. This problem is of fundamental importance as it provides the exact solution and reveals how the velocity profile varies with time approaching a linear distribution asymptotically, and how the boundary layer spread throughout the flow field.

**Manuscript Received on August 2014.**

**S. Harisingh Naik**, Department of Mathematics and Computer Science University College of Science, Osmania University, Hyderabad-500007, India.

**K. Rama Rao**, Department of Mathematics, Chaithanya Bharathi Institute of Technology (C. B. I. T), Gandipet, Hyderabad, 500075, Andhra Pradesh, India.

**M. V. Ramana Murthy**, Department of Mathematics and Computer Science University College of Science, Osmania University, Hyderabad-500007, India.

Free convection in vertical channels has been studied widely in the last few decades under different physical effects [10] – [16] due to its importance in many engineering applications such as cooling of electronic equipments, design of passive solar systems for energy conversion, cooling of nuclear reactors, design of heat exchangers, chemical devices and process equipment, geothermal systems, and others. However, very few papers deal with free convection in Couette motion between vertical parallel plates. Singh [17] studied the effect of free convection in Couette motion. He has considered the unsteady free convective flow of a viscous incompressible fluid between two vertical parallel plates at constant but different temperatures and one of which is impulsively started in its own plane and the other is kept stationary. This problem was further extended for magneto hydrodynamic case by Jha [18]. Fully developed laminar free convection Couette flow between two vertical parallel plates with transverse sinusoidal injection of the fluid at the stationary plate and its corresponding removal by constant suction through the plate in uniform motion has been analyzed by Jain and Gupta [19]. The physical effect of external shear in the form of Couette flow of a Bingham fluid in a vertical parallel plane channel with constant temperature differential across the walls was investigated analytically by Barletta and Magyari [20]. Steady fully developed combined forced and free convection Couette flow with viscous dissipation in a vertical channel has been investigated analytically by Barletta *et al.* [21]. In their study, the moving wall is thermally insulated and the wall at rest is kept at a uniform temperature. The fluids that are used extensively in industrial applications are exhibiting a yield stress  $\tau_0$ , that has to be exceeded before the fluid moves. As a result, such fluids cannot sustain a velocity gradient unless the magnitude of the local shear stress is higher than this yield stress. Fluids that belong to this category include cement, drilling mud, sludge, grease, granular suspensions, aqueous foams, slurries, paints, food products, plastics and paper pulp [22]. Due to the growing use of these non-Newtonian materials in various manufacturing and processing industries, considerable efforts have been directed towards understanding their flow and heat transfer characteristics. Many of the yield non-Newtonian fluids encountered in chemical engineering processes, are known to follow the so – called “Bingham model”. A Bingham fluid is a material with a finite yield stress, followed by a linear curve at a finite strain rate. Many authors [23]–[27] studied the flow/and heat transfer of a Bingham fluid in different geometries. Thermal radiation effects on hydro magnetic free convection flow play an important role in manufacturing processes taking place in industries for the

design of fins, glass production, steel rolling, casting and Morevoer, several engineering processes occur at very high temperatures where the knowledge of radioactive heat transfer becomes indispensable for the design of pertinent equipment. Nuclear power plants, gas turbines and various propulsion devices for aircraft, missiles, satellites and space vehicles are examples of such engineering areas [28]. It is worthy to note that unlike convection/conduction the governing equations taking into account the effects of thermal radiation become quite complicated. Hence many difficulties arise while solving such equations. However, some reasonable approximations are proposed to solve the governing equations with radioactive heat transfer. Viskanta and Grosh [29] were one of the initial investigators to study the effects of thermal radiation on temperature distribution and heat transfer in an absorbing and emitting media flowing over a wedge. They used Roseland approximation for the radioactive flux vector to simplify the energy equation. Cess [30] studied laminar free convection along a vertical isothermal plate with thermal radiation. The text books by Sparrow and Cess [31] and Howell *et al.* [32] present the most essential features and state of the art applications of radioactive heat transfer. Takhar *et al.* [33] analyzed the effects of radiation on MHD free convection flow of a gas past a semi – infinite vertical plate. Raptis and Massalas [34] studied oscillatory magneto hydrodynamic flow of a gray, absorbing-emitting fluid with non-scattering medium past a flat plate in the presence of radiation assuming the Roseland flux model. Chamkha [35] discussed thermal radiation and buoyancy effects on hydro magnetic flow over an accelerating permeable surface with heat source or sink. Cookey *et al.* [36] considered the influence of viscous dissipation and radiation on unsteady MHD free convection flow past an infinite heated vertical plate in a porous medium with time-dependent suction. Ogulu and Makinde [37] considered unsteady hydro magnetic free convection flow of a dissipative and radioactive fluid past a vertical plate with constant heat flux. Mahmoud [38] investigated the effects of thermal radiation on unsteady MHD free convection flow past an infinite vertical porous plate taking into account the effects of viscous dissipation. It is noticed that when the density of an electrically conducting fluid is low and/or applied magnetic field is strong, Hall current is produced in the flow field which plays an important role in determining flow features of the problems because it induces secondary flow in the flow field. Keeping in view this fact, significant investigations on hydro magnetic free convection flow past a flat plate with Hall effects under different thermal conditions are carried out by several researchers in the past. Mention may be made of the research studies of Pop and Watanabe [39], Abo – Eldahab and Elbarbary [40], Takhar *et al.* [41] and Saha *et al.* [42]. It is worthy to note that Hall current induces secondary flow in the flow field which is also the characteristics of Coriolis force. Therefore, it becomes very important to compare and contrast the effects of these two agencies and also to study their combined effects on such fluid flow problems. Satya Narayana *et al.* [43] studied the effects of Hall current and radiation-absorption on MHD natural convection heat and mass transfer flow of a micro polar fluid in a rotating frame induced magnetic field is neglected by assuming a very small magnetic Reynolds number. The Hall Effect is taken

levitation, furnace design, etc. of reference. Seth *et al.* [44] investigated effects of Hall current and rotation on unsteady hydro magnetic natural convection flow of a viscous, incompressible, electrically conducting and heat absorbing fluid past an impulsively moving vertical plate with ramped temperature in a porous medium taking into account the effects of thermal diffusion. The aim of the present paper is to find numerical solutions of unsteady magneto hydrodynamic the numerical solution of unsteady magneto hydrodynamic flow of an electrically conducting viscous incompressible non – Newtonian Bingham fluid bounded by two parallel non – conducting porous plates is studied with thermal radiation considering the Hall Effect. The dimensionless governing coupled, non – linear boundary layer partial differential equations are solved by an efficient, accurate, and extensively validated and unconditionally stable finite difference scheme of the Crank – Nicolson method, which is more economical from a computational point of view. These solutions are useful to gain a deeper knowledge of the underlying physical processes and it provides the possibility to get a benchmark for numerical solvers with reference to basic flow configurations. The behavior of the velocity, temperature, skin – friction coefficient and Nusselt number has been discussed in detail for variations in the physical parameters. In section 2, the mathematical formulation of the problem and dimension less forms of the governing equations are established. Solution method to these equations for the flow variables are briefly examined in section 3. The results of the previous sections are discussed in section 4. In section 5, general concluding remarks of the results of the previous sections are given.

## II. MATHEMATICAL FORMULATION

The unsteady magneto hydrodynamic flow of an electrically conducting viscous incompressible non – Newtonian Bingham fluid bounded by two parallel non – conducting porous plates with thermal radiation considering the Hall Effect is studied.

1. The fluid is assumed to be laminar, incompressible and obeying a Bingham model and flows between two infinite horizontal plates located at the  $y' = \pm h$  planes and extend from  $x' = 0$  to  $\infty$  and from  $z' = 0$  to  $\infty$ .
2. The upper plate moves with a uniform velocity  $U_0$  while the lower plate is stationary. The upper and lower plates are kept at two constant temperatures  $T_2'$  and  $T_1'$  respectively with  $T_2' > T_1'$ .
3. The fluid is acted upon by a constant pressure gradient  $\frac{dp'}{dx'}$  in the  $x'$  – direction, and a uniform suction from above and injection from below which are applied at  $t' > 0$ .
4. A uniform magnetic field  $B_0$  is applied in the positive  $y'$  – direction and is assumed undisturbed as the

into consideration and consequently a  $z'$  – component for the velocity is expected to arise.

5. It is assumed that the external electric field is zero and the electric field due to the polarization of charges is negligible.
6. The homogeneous chemical reaction of first order with rate constant between the diffusing species and the fluid is neglected.
7. The concentration of the diffusing species in the binary mixture is assumed to be very small in comparison with the other chemical species, which are present and hence Soret and Dufour effects are negligible.
8. The uniform suction implies that the  $y$  – component of the velocity is constant. Thus, the fluid velocity vector is given by  

$$v(y', t') = u'(y', t')\bar{i} + v_o\bar{j} + w'(y', t')\bar{k}$$

injection, the problem reduces to Poiseuille problem [45] the classical hydrodynamic linear problem. Without suction – injection and by neglecting the Hall current, it reduces to Hartmann – Poiseuille problem [46], the classical MHD linear problem. The inclusion of the constant suction – injection as well as the Hall term [47] preserves linearity. So obviously does changing the Newtonian fluid to a non – Newtonian one in the present study. The classical problems (Poiseuille and Hartmann – Poiseuille) of channel flow and the related pipe flow of Newtonian fluid are known to be attainable in practice and to give results in excellent agreement with experiments. The fully developed profiles are observed away from the inlet and the side – walls of the channel. Using a non – Newtonian fluid is not expected to cause a problem.

It should be noted that the problem comes out to be a linear problem. In the hydrodynamic case without suction –

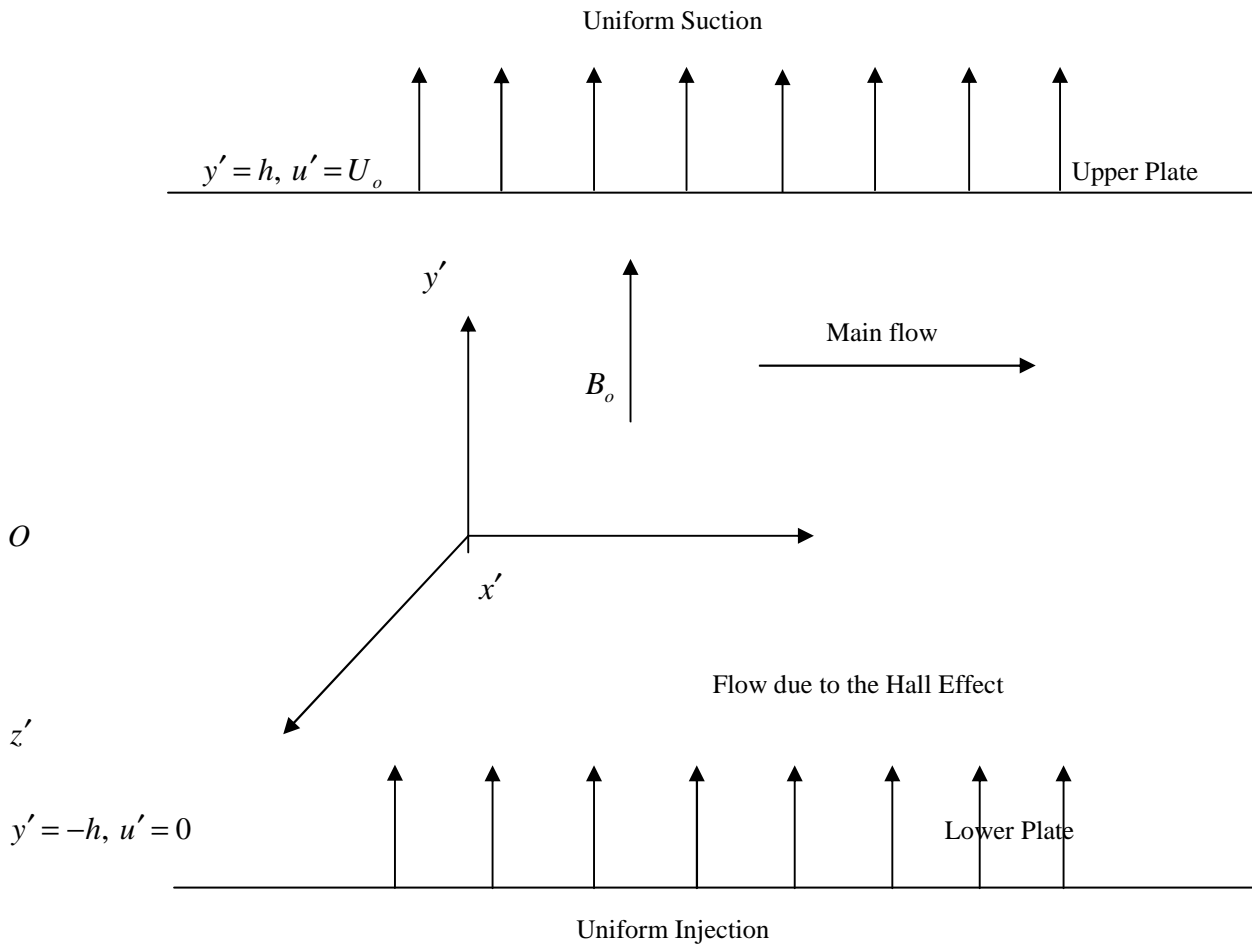


**Figure 1. Geometry of the Problem**

Using a non – Newtonian fluid is not expected to cause a problem. The fluid motion starts from rest at  $t' = 0$ , and the no – slip condition at the plates implies that the fluid velocity has neither a  $z'$  nor an  $x'$  – component at  $y' = \pm h$ . The initial temperature of the fluid is assumed to be equal to  $T_1'$ . Since the plates are infinite in the  $x'$  and  $z'$  directions, the physical quantities do not change in these directions. The flow of the fluid is governed by the momentum equation

$$\rho \frac{Dv}{Dt'} = \nabla \cdot (\mu \nabla v) - \nabla p' + \bar{J} \times B_o \quad (1)$$

Where  $\rho$  the density of the fluid and  $\mu$  is the apparent viscosity of the model and is given by

$$u' = K + \frac{\tau_o}{\sqrt{\left(\frac{\partial u'}{\partial y'}\right)^2 + \left(\frac{\partial w'}{\partial y'}\right)^2}} \quad (2)$$

Where  $K$  the plastic viscosity of a Bingham fluid,  $\tau_o$  is the yield stress. If the Hall term is retained, the current density

$\bar{J}$  is given by

$$\bar{J} = \sigma[v \times B_o - \beta(\bar{J} \times B_o)] \quad (3)$$

Where  $\sigma$  is the electric conductivity of the fluid and  $\beta$  is the Hall factor. Equation (3) may be solved in  $\bar{J}$  to yield

$$\bar{J} \times B_o = -\frac{\sigma B_o^2}{1+m^2} [(u' + mw')\bar{i} + (w' - mu')\bar{k}] \quad (4)$$

Where  $m$  is the Hall parameter and  $m = \sigma\beta B_o$ . Thus, the two components of the momentum equation (1) read

$$\rho C_p \frac{\partial T'}{\partial t'} + \rho C_p v_o \frac{\partial T'}{\partial y'} = \kappa \frac{\partial}{\partial y'} \left( \frac{\partial T'}{\partial y'} \right) + \mu \left[ \left( \frac{\partial u'}{\partial y'} \right)^2 + \left( \frac{\partial w'}{\partial y'} \right)^2 \right] + \frac{\sigma B_o^2}{1+m^2} (u'^2 + w'^2) - \frac{\partial q_r}{\partial y'} \quad (7)$$

Where  $C_p$ ,  $\kappa$  and  $D$  are respectively, the specific heat capacity, the thermal conductivity and thermal diffusivity of the fluid. The second and third terms on the right – hand side of (7) represent the viscous and Joule dissipations respectively. We notice that each of these terms has two components. This is because the Hall Effect brings about a velocity  $w'$  in the  $z'$  – direction.

The radioactive heat flux term is simplified by making use of the Roseland approximation [48] as  $q_r = -\frac{4\bar{\sigma}}{3k^*} \frac{\partial T'^4}{\partial y'}$

(8)

Here  $\bar{\sigma}$  is Stefan – Boltzmann constant and  $k^*$  is the mean absorption coefficient. It is assumed that the temperature differences within the flow are sufficiently small so that

$$\rho C_p \frac{\partial T'}{\partial t'} + \rho C_p v_o \frac{\partial T'}{\partial y'} = \kappa \frac{\partial}{\partial y'} \left( \frac{\partial T'}{\partial y'} \right) + \mu \left[ \left( \frac{\partial u'}{\partial y'} \right)^2 + \left( \frac{\partial w'}{\partial y'} \right)^2 \right] + \frac{\sigma B_o^2}{1+m^2} (u'^2 + w'^2) + \frac{16\bar{\sigma}T_1^{\delta}}{3k^*} \frac{\partial^2 T'}{\partial y'^2} \quad (11)$$

The initial and boundary conditions of the problem are given by

$$\left\{ \begin{array}{l} t' \leq 0 : u' = w' = 0, T' = T_1' \text{ for all } y' \\ t' > 0 : \begin{cases} u' = w' = 0, T' = T_1' \text{ at } y' = -h \\ u' = U_o, w' = 0, T' = T_2' \text{ at } y' = h \end{cases} \end{array} \right. \quad (12)$$

That the boundary conditions do not show dependence on  $x'$  suggests that the problem has a fully developed solution of the form:

$$x = \frac{x'}{h}, \quad y = \frac{y'}{h}, \quad z = \frac{z'}{h}, \quad t = \frac{t'U_o}{h}, \quad u = \frac{u'}{U_o}, \quad w = \frac{w'}{U_o}, \quad p = \frac{p'}{\rho U_o^2}, \quad \theta = \frac{T' - T_1'}{T_2' - T_1'}, \quad \bar{\mu} = \frac{\mu}{K}, \quad \tau_D = \frac{\tau_o h}{KU_o} \text{ is the}$$

$$\rho \frac{\partial u'}{\partial t'} + \rho v_o \frac{\partial u'}{\partial y'} = -\frac{\partial p'}{\partial x'} + \frac{\partial}{\partial y'} \left( \mu \frac{\partial u'}{\partial y'} \right) - \frac{\sigma B_o^2}{1+m^2} (u' + mw') \quad (5)$$

$$\rho \frac{\partial w'}{\partial t'} + \rho v_o \frac{\partial w'}{\partial y'} = \frac{\partial}{\partial y'} \left( \mu \frac{\partial w'}{\partial y'} \right) - \frac{\sigma B_o^2}{1+m^2} (w' - mu') \quad (6)$$

Where  $\frac{\partial p'}{\partial x'} = \frac{dp'}{dx'} e^{-at}$  is the unsteady pressure gradient.

The energy equation with viscous and Joule dissipations is given by

$$T'^4 \text{ can be expressed as a linear function of } T' \text{ after using Taylor's series to expand } T'^4 \text{ about the free stream temperature } T_1' \text{ and neglecting higher – order terms. This results in the following approximation:}$$

$T'^4 \cong 4T_1^{\delta} T' - 3T_1^4$

Using equations (8) and (9) in the last term of equation (7), we obtain:

$$\frac{\partial q_r}{\partial y'} = -\frac{16\bar{\sigma}T_1^{\delta}}{3k^*} \frac{\partial^2 T'}{\partial y'^2} \quad (10)$$

Introducing (10) in the equation (7), the energy equation becomes:

$$u' = u'(y', t'), \quad v = v_o, \quad p' = P + Gx'$$

Where  $P$  is the pressure at  $x' = 0$  (constant),  $G$  is the constant pressure gradient (negative). Under these conditions the continuity equation  $\left( \frac{\partial u'}{\partial x'} + \frac{\partial v'}{\partial y'} = 0 \right)$  is

automatically satisfied. It is expedient to write the above equations in the non – dimensional form. To do this, we introduce the following non – dimensional quantities

Bingham Number (Dimensionless yield stress),  $\alpha = \frac{dp'}{dx'}$  is the pressure gradient,

$Re = \frac{\rho U_o h}{K}$  is the Reynolds number,  $S = \frac{\rho v_o h}{K}$  is the suction parameter,

$Pr = \frac{\rho C_p U_o h}{K}$  is the Prandtl number,

$Ec = \frac{U_o K}{\rho C_p h (T'_2 - T'_1)}$  is the Eckert number,

$$\frac{\partial u}{\partial t} + \frac{S}{Re} \frac{\partial u}{\partial y} = -\frac{dp}{dx} + \frac{1}{Re} \left[ \frac{\partial}{\partial y} \left( \mu \frac{\partial u}{\partial y} \right) - \frac{M^2}{1+m^2} (u + mw) \right] \quad (13)$$

$$\frac{\partial w}{\partial t} + \frac{S}{Re} \frac{\partial w}{\partial y} = \frac{1}{Re} \left[ \frac{\partial}{\partial y} \left( \mu \frac{\partial w}{\partial y} \right) - \frac{M^2}{1+m^2} (w - mu) \right] \quad (14)$$

$$\frac{\partial \theta}{\partial t} + \frac{S}{Re} \frac{\partial \theta}{\partial y} = \frac{1}{Pr} \left( \frac{3R+4}{3R} \right) \frac{\partial}{\partial y} \left( \frac{\partial \theta}{\partial y} \right) + (Ec) \mu \left[ \left( \frac{\partial u}{\partial y} \right)^2 + \left( \frac{\partial w}{\partial y} \right)^2 \right] + \frac{M^2 (Ec)}{1+m^2} (u^2 + w^2) \quad (15)$$

And the corresponding boundary conditions are

$$\left\{ \begin{array}{l} t \leq 0 : u = w = \theta = 0 \quad \text{for all } y \\ t > 0 : \begin{cases} u = w = \theta = 0 \quad \text{at } y = -1 \\ u = 1, w = 0, \theta = 1 \quad \text{at } y = 1 \end{cases} \end{array} \right\} \quad (16)$$

$$\text{Where } \mu = 1 + \frac{\tau_D}{\sqrt{\left( \frac{\partial u}{\partial y} \right)^2 + \left( \frac{\partial w}{\partial y} \right)^2}} \quad (17)$$

$$\text{and } \frac{dp}{dx} = \alpha e^{-at} \quad (18)$$

### III. NUMERICAL SOLUTION BY CRANK-NICHOLSON METHOD

Equations (13), (14), (17) represent coupled system of non-linear partial differential equations which are solved numerically under the initial and boundary conditions (16) using the finite difference approximations. A linearization technique is first applied to replace the non-linear terms at a linear stage, with the corrections incorporated in subsequent iterative steps until convergence is reached. Then the Crank-Nicolson implicit method is used at two successive time levels [49]. An iterative scheme is used to solve the linearized system of difference equations. The solution at a certain time step is chosen as an initial guess for next time step and the iterations are continued till convergence, within a prescribed accuracy. Finally, the resulting block tridiagonal system is solved using the generalized Thomas-algorithm [49]. The energy equation (15) is a linear non-homogeneous second order partial differential equation whose right hand side is known from

$R = \frac{\kappa k^*}{4\sigma T_1'^3}$  is the thermal radiation parameter and

$M^2 = \frac{\sigma B_o^2 h^2}{K}$  is the Hartmann number squared.

In terms of the above non-dimensional variables and parameters equations (5) – (6) and (11) are, respectively, written as (where the hats are dropped for convenience)

the solutions of the flow Equations (13), (14), (17) subject to the conditions (16). The values of the velocity components are substituted in the right hand side of equation (15) which is solved numerically with the initial and boundary conditions (16) using central differences and Thomas algorithm to obtain the temperature distribution. Finite difference equations relating the variables are obtained by writing the equations at the midpoint of the computational cell and then replacing the different terms by their second order central difference approximations in the  $y$ -direction. The diffusion terms are replaced by the average of the central differences at two successive time-levels. The computational domain is divided into meshes of dimension  $\Delta t$  and  $\Delta y$  in time and space respectively as shown in figure 2. We define the variables  $B = u_y$ ,  $D = w_y$ ,  $L = \theta_y$  and  $\bar{\mu} = \mu_y$  to reduce the second order differential equations (13), (14), (17) to first order differential equations. The finite difference

representations for the resulting first order differential equations (13), (14) take the following forms:

$$\left(\frac{u_{i+1,j+1} - u_{i,j+1} + u_{i+1,j} - u_{i,j}}{2(\Delta t)}\right) + \frac{S}{\text{Re}} \left(\frac{B_{i+1,j+1} + B_{i,j+1} + B_{i+1,j} + B_{i,j}}{4}\right) = -\alpha e^{at} + \left(\frac{\bar{\mu}_{i+\frac{1}{2},j+\frac{1}{2}}}{\text{Re}}\right)$$

$$\left(\frac{(B_{i+1,j+1} + B_{i,j+1}) - (B_{i+1,j} + B_{i,j})}{2(\Delta y)}\right) + \left(\frac{\bar{\mu}'_{i+\frac{1}{2},j+\frac{1}{2}}}{\text{Re}}\right) \left(\frac{B_{i+1,j+1} + B_{i,j+1} + B_{i+1,j} + B_{i,j}}{4}\right) -$$
(19)

$$\left(\frac{M^2}{1+m^2}\right) \left\{ \left(\frac{u_{i+1,j+1} + u_{i,j+1} + u_{i+1,j} + u_{i,j}}{4\text{Re}}\right) + m \left(\frac{w_{i+1,j+1} + w_{i,j+1} + w_{i+1,j} + w_{i,j}}{4\text{Re}}\right) \right\}$$

$$\left(\frac{w_{i+1,j+1} - w_{i,j+1} + w_{i+1,j} - w_{i,j}}{2(\Delta t)}\right) + \frac{S}{\text{Re}} \left(\frac{D_{i+1,j+1} + D_{i,j+1} + D_{i+1,j} + D_{i,j}}{4}\right) = \left(\frac{\bar{\mu}_{i+\frac{1}{2},j+\frac{1}{2}}}{\text{Re}}\right)$$

$$\left(\frac{(D_{i+1,j+1} + D_{i,j+1}) - (D_{i+1,j} + D_{i,j})}{2(\Delta y)}\right) + \left(\frac{\bar{\mu}'_{i+\frac{1}{2},j+\frac{1}{2}}}{\text{Re}}\right) \left(\frac{D_{i+1,j+1} + D_{i,j+1} + D_{i+1,j} + D_{i,j}}{4}\right) -$$
(20)

$$\left(\frac{M^2}{1+m^2}\right) \left\{ m \left(\frac{u_{i+1,j+1} + u_{i,j+1} + u_{i+1,j} + u_{i,j}}{4\text{Re}}\right) - \left(\frac{w_{i+1,j+1} + w_{i,j+1} + w_{i+1,j} + w_{i,j}}{4\text{Re}}\right) \right\}$$

Where  $\bar{\mu}_{i+\frac{1}{2},j+\frac{1}{2}} = \frac{\bar{\mu}_{i+1,j+1} + \bar{\mu}_{i+1,j} + \mu_{i,j+1} + \mu_{i,j}}{4}$  and  $\bar{\mu}'_{i+\frac{1}{2},j+\frac{1}{2}} = \frac{\bar{\mu}'_{i+1,j+1} + \bar{\mu}'_{i+1,j} + \mu'_{i,j+1} + \mu'_{i,j}}{4}$

(21)

The variables with bars are given initial guesses from the previous time step and an iterative scheme is used at every time to solve the linearized system of difference equations. Then the finite difference form for the energy equation (15) can be written as

$$\left(\frac{\theta_{i+1,j+1} - \theta_{i,j+1} + \theta_{i+1,j} - \theta_{i,j}}{2(\Delta t)}\right) + \frac{S}{\text{Re}} \left(\frac{L_{i+1,j+1} + L_{i,j+1} + L_{i+1,j} + L_{i,j}}{4}\right) =$$

$$\frac{1}{\text{Pr}} \left(\frac{3R+4}{3R}\right) \left(\frac{(L_{i+1,j+1} + L_{i,j+1}) - (L_{i+1,j} + L_{i,j})}{4}\right) + QZFO$$
(22)

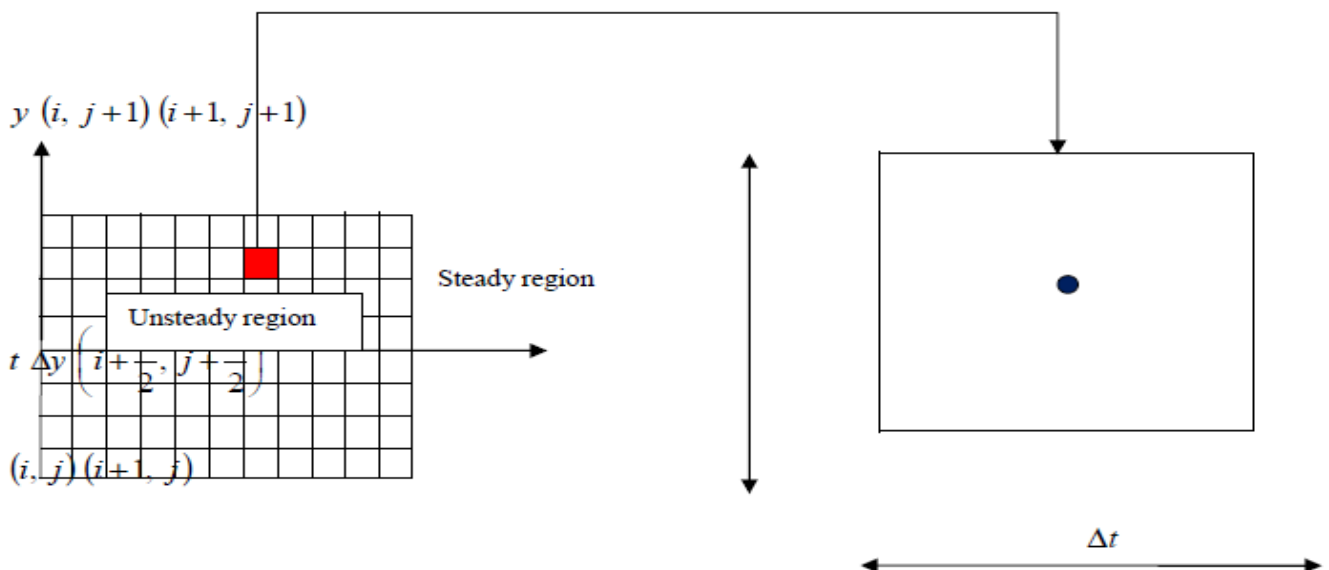


Figure 2. Mesh Layout

Where  $QZFO$  represents the Joule and viscous dissipation terms which are known from the solution of the momentum equations and can be evaluated at the midpoint  $\left(i + \frac{1}{2}, j + \frac{1}{2}\right)$  of the computational cell. Computations have been made for  $\alpha = 2.0$ ,  $Pr = 0.71$ ,  $Re = 2.0$ ,  $M = 2.0$ ,  $Ec = 0.03$  and  $R = 2.0$ . Grid – independence studies show that the computational domain  $0 < t < \infty$  and  $-1 < y < 1$  can be divided into intervals with step sizes  $\Delta t = 0.0001$  and  $\Delta y = 0.005$  for time and space respectively. The truncation error of the central difference schemes of the governing equations is  $O(\Delta t^2, \Delta y^2)$ . Stability and rate of convergence are functions of the flow and heat parameters. Smaller step sizes do not show any significant change in the results. Convergence of the scheme is assumed when all of the unknowns  $u$ ,  $B$ ,  $w$ ,  $D$ ,  $\theta$  and  $L$  for the last two approximations differ from unity by less than  $10^{-6}$  for all values of  $y$  in  $-1 < y < 1$  at every time step. Less than 7 approximations are required to satisfy this convergence criteria for all ranges of the parameters studied here.

#### IV. RESULTS AND DISCUSSIONS

Figures (3) – (5) present the profiles of the velocity components  $u$  and  $w$  and the temperature  $\theta$  respectively for various values of time  $t$  and for  $\tau_D = 0, 0.05$ , and  $0.1$ . The figures are evaluated for  $M = 3.0$ ,  $m = 3.0$ ,  $S = 1.0$  and  $R = 2.0$ . It is clear from figures (3) and (4) that increasing the yield stress  $\tau_D$  decreases the velocity components  $u$  and  $w$  and the time at which they reach their steady state values as a result of increasing the viscosity. The figures show also that the velocity components  $u$  and  $w$  do not reach their steady state monotonically. Both  $u$  and  $w$  increase with time up till a maximum value and then decrease up to the steady state. This behavior is more pronounced for small values of the parameter  $\tau_D$  and it is more clear for  $u$  than for  $w$ . Figure (5) shows that the temperature profile reaches its steady state monotonically. It is observed also that the velocity component  $u$  reaches the

steady state faster than  $w$  which, in turn, reaches the steady state faster than  $\theta$ . This is expected as  $u$  is the source of  $w$ , while both  $u$  and  $w$  act as sources for the temperature. Figures (6) – (8) depict the variation of the velocity components  $u$  and  $w$  and the temperature  $\theta$  at the centre of the channel ( $y = 0$ ) with time respectively for various values of the Hall parameter  $m$  and for  $\tau_D = 0, 0.05$ , and  $0.1$ . In these figures  $M = 3.0$  and  $S = 1.0$ . Fig. 6 shows that  $u$  increases with increasing  $m$  for all values of  $\tau_D$  as the effective conductivity  $\left(= \sigma / (1 + m^2)\right)$  decreases with increasing  $m$  which reduces the magnetic damping force on  $u$ . It is observed also from the figure that the time at which  $u$  reaches its steady state value increases with increasing  $m$  while it decreases when  $\tau_D$  increases. The effect of  $\tau_D$  on  $u$  becomes more pronounced for large values of  $m$ . In figure (7) the velocity component  $w$  increases with increasing  $m$  as  $w$  is a result of the Hall Effect. On the other hand, at small times,  $w$  decreases when  $m$  increases. This happens due to the fact that, at small times  $w$  is very small and then the source term of  $w$  is proportional to  $\left(mu / (1 + m^2)\right)$  which decreases with increasing  $m$  ( $m > 1$ ). This accounts for the crossing of the curves of  $w$  with  $t$  for all values of  $\tau_D$ . Figures (6) and (7) indicate also that the influence of  $\tau_D$  on  $u$  and  $w$  depends on  $m$  and becomes more clear when  $m$  is large. An interesting phenomenon is observed in Figures (6) and (7), which is that, when  $m$  has a non – zero value the component  $u$  and, sometimes,  $w$  overshoot. For some times they exceed their steady state values and then go down towards steady state. This may be explained by stating that with the progress of time,  $u$  increases and consequently  $w$  increases according to equation (11) until  $w$  reaches its maximum value. The increase in  $w$  results in a small decrease in  $u$  according to equation (10). This reduction in  $u$  may, in turn, result in a decrease in  $w$  according to equation (11) which explains the reduction after the peaks. The time at which overshooting occurs decreases with increasing  $\tau_D$ . Figure (8) shows that the influence of  $m$  on  $\theta$  depends on  $t$ . Increasing  $m$

decreases  $\theta$  at small times and increases it at large times. This is due to the fact that, for small times,  $u$  and  $w$  are small and an increase in  $m$  increases  $u$  but decreases  $w$ . Then, the Joule dissipation which is also proportional to  $(1/(1+m^2))$  decreases. For large times, increasing  $m$  increases both  $u$  and  $w$  and, in turn, increases the Joule and viscous dissipations. This accounts for the crossing of the curves of  $\theta$  with time for all values of  $\tau_D$ . It is also observed that increasing  $\tau_D$  decreases the temperature  $\theta$  for all values of  $m$ . This is because increasing  $\tau_D$  decreases both  $u$  and  $w$  and their gradients which decreases the Joule and viscous dissipations. The figure shows also that the time at which  $\theta$  reaches its steady state value increases with increasing  $m$  while it is not greatly affected by changing  $\tau_D$ . Figures(9) – (11) show the effect of the suction parameter  $S$  on the time development of the velocity components  $u$  and  $w$  and the temperature  $\theta$  at  $y = 0$  with time respectively for various values for  $\tau_D = 0.0, 0.05, \text{ and } 0.1$ . In these figures  $M = 3.0$  and  $m = 3.0$ . Figure (9) shows that  $u$  at the centre of the channel decreases with increasing  $S$  for all values of  $\tau_D$  due to the convection of the fluid from regions in the lower half to the centre, which has higher fluid speed. Figure (10) overshooting in  $w$  especially for small values of  $\tau_D$ . Figure (11) indicates that increasing  $S$  decreases the

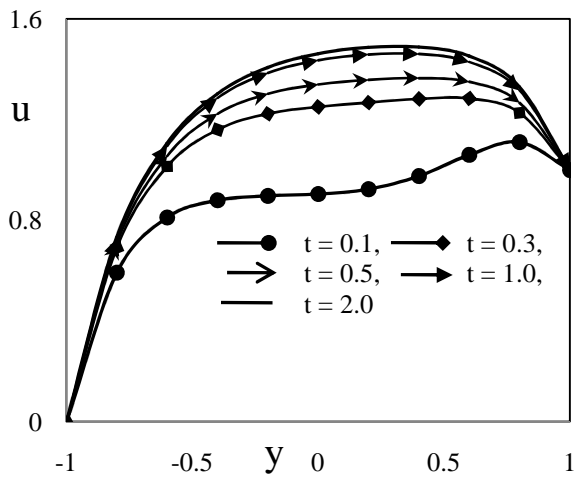
temperature at the centre of the channel for all values of  $\tau_D$ . This is due to the influence of the convection in pumping the fluid from the cold lower half towards the centre of the channel. Figures (12) – (14) show the effect of the thermal radiation parameter  $R$  on the time development of the velocity components  $u$  and  $w$  and the temperature  $\theta$  at  $y = 0$  with time respectively for various values for  $\tau_D = 0.0, 0.05, \text{ and } 0.1$ . In these figures  $m = 3, M = 3$  and  $S = 1$ . It is observed that increasing  $R$  decreases the velocity components and temperature of the fluid. An increase in the radiation emission, which is represented by  $R$ , reduces the rate of heat transfer through the fluid. This accounts for the decrease in temperature with increasing  $R$ . The velocity components are decreases through there diction in buoyancy forces associated with the decreased temperature. In order to examine the accuracy and correctness of the solutions, the results of the time development of the velocity components  $u$  and  $w$  at the centre of the channel for the Newtonian case is compared and shown, as depicted Table – 1, to have complete agreement with those reported by Attia [50]. This ensures the satisfaction of all the governing equations; mass continuity, momentum and energy equations. While comparisons with previously published theoretical work on this problem were performed, no comparisons with experimental data were done because, as far as the author is aware, such data are lacking at the present time.

**Table 1. Comparison of the Present Results and the Known Results of Attia [50] for Newtonian Fluid ( $\tau_D = 0.0$ ) and**

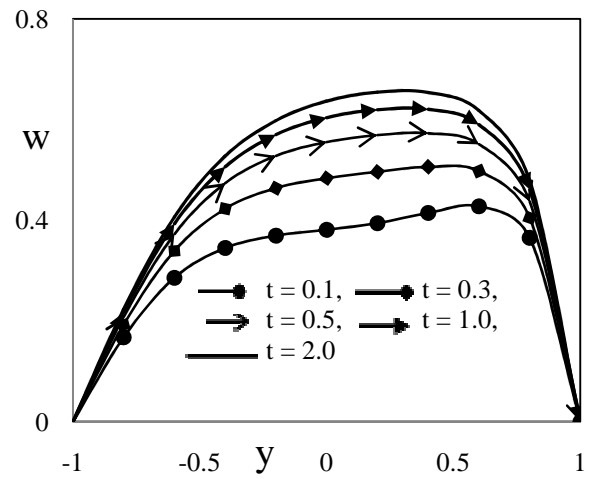
**$R = 0$  for  $m = 3, M = 3, S = 1$  and  $y = 0$**

$t$	Values of $u$		Values of $w$	
	Present results	Attia [50]	Present results	Attia [50]
0.1	0.4678	0.4669	0.0627	0.0619
0.2	0.8093	0.8089	0.2069	0.2056
0.3	1.0171	1.0160	0.3699	0.3687
0.4	1.1267	1.1251	0.5184	0.5171
0.5	1.1722	1.1708	0.6378	0.6370
0.6	1.1801	1.1791	0.7262	0.7260
0.7	1.1689	1.1682	0.7873	0.7872
0.8	1.1510	1.1495	0.8266	0.8263
0.9	1.1305	1.1297	0.8501	0.8491
1.0	1.1129	1.1122	0.8615	0.8607

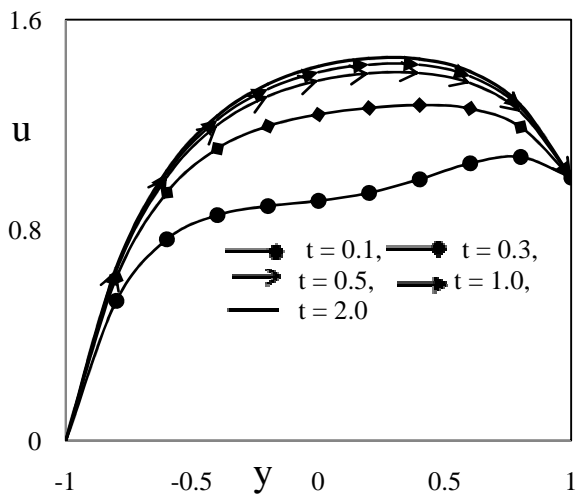




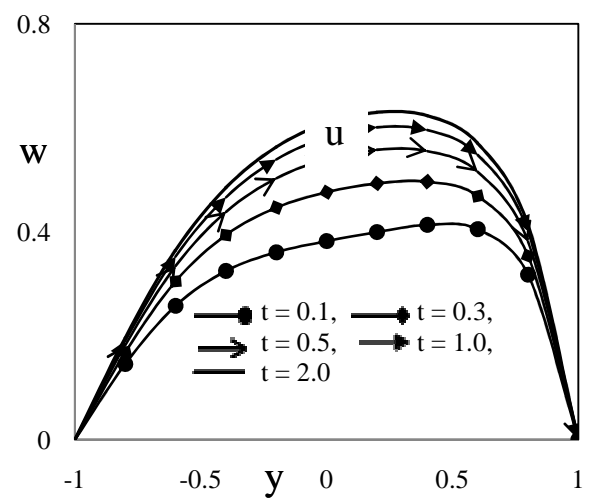
(a)  $\tau_D = 0.0$



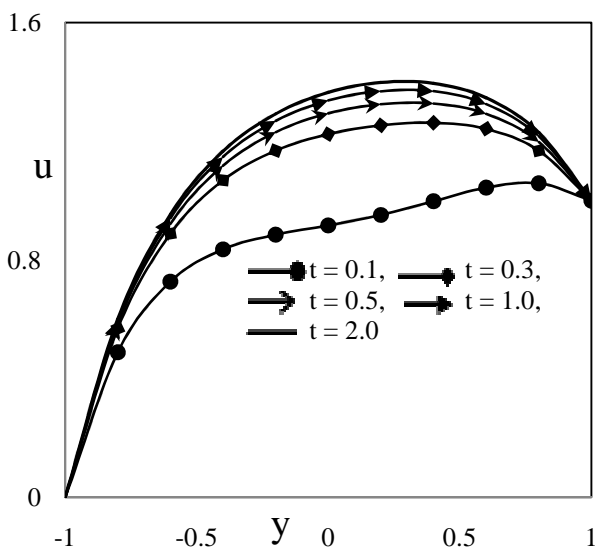
(a)  $\tau_D = 0.0$



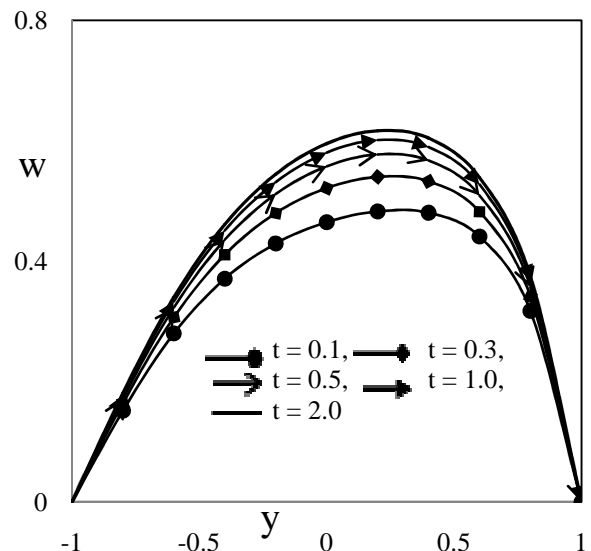
(b)  $\tau_D = 0.05$



(b)  $\tau_D = 0.05$



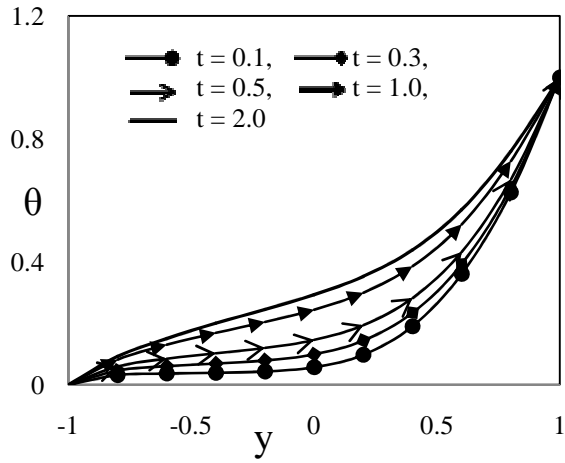
(c)  $\tau_D = 0.10$



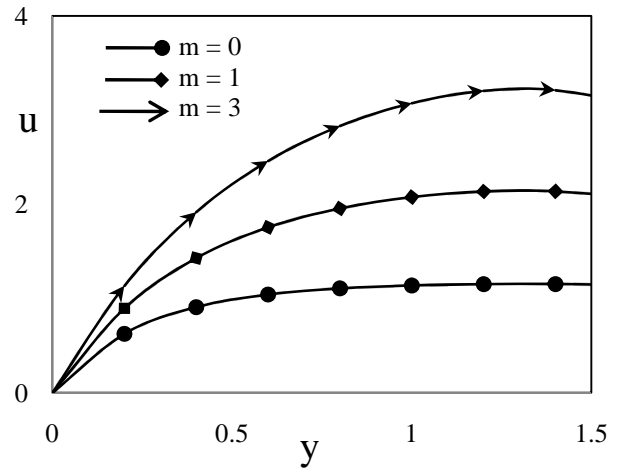
(c)  $\tau_D = 0.10$

Figure 3. Time Development of the Velocity Component  $u$  for  $S = 1$ ,  $M = 3$  and  $R = 2$

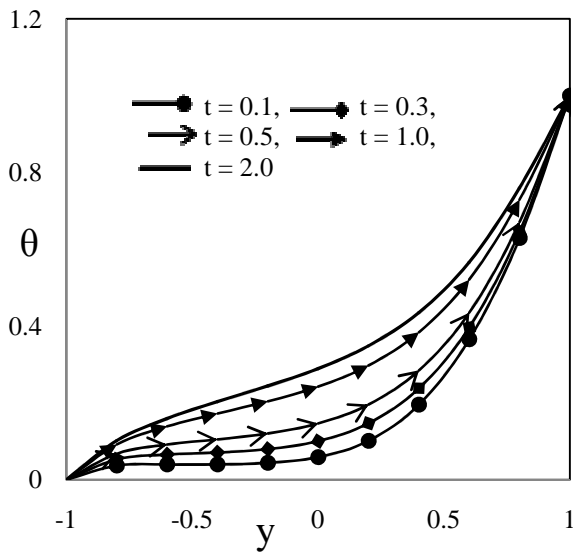
Figure 4. Time Development of the Velocity Component  $w$  for  $S = 1$ ,  $M = 3$ ,  $m = 3$  and  $R = 2$



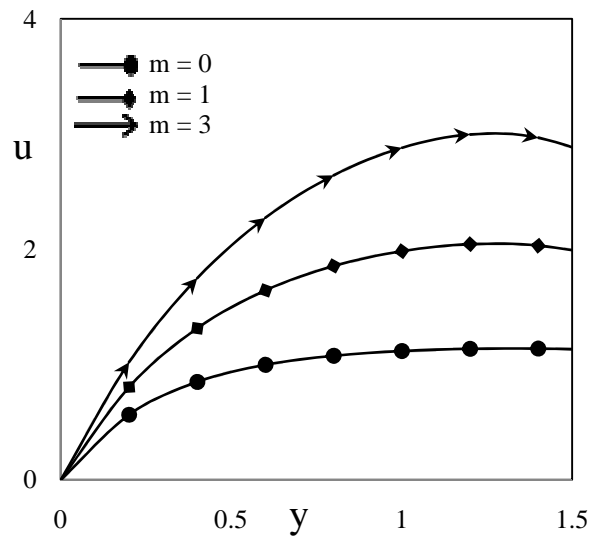
(a)  $\tau_D = 0.0$



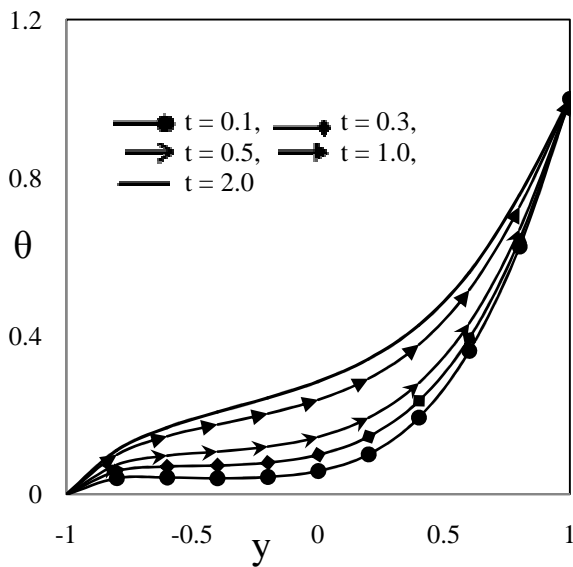
(a)  $\tau_D = 0.0$



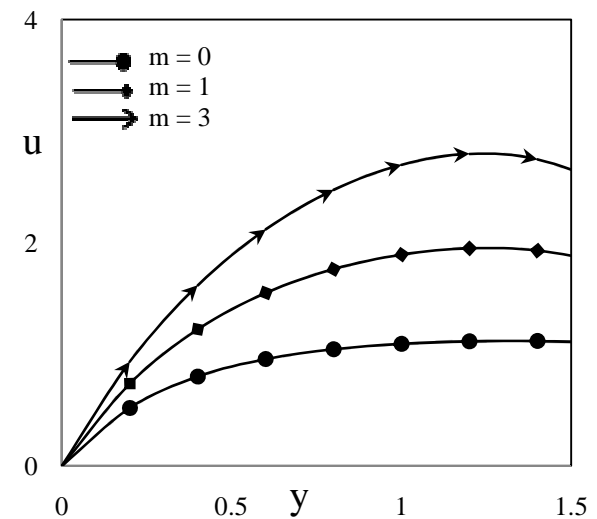
(b)  $\tau_D = 0.05$



(b)  $\tau_D = 0.05$



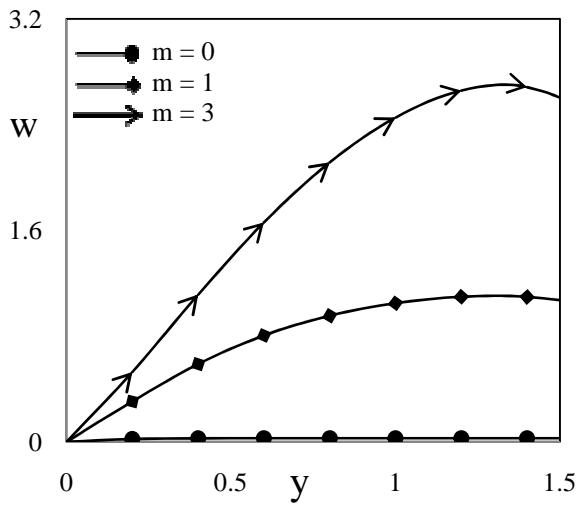
(c)  $\tau_D = 0.10$



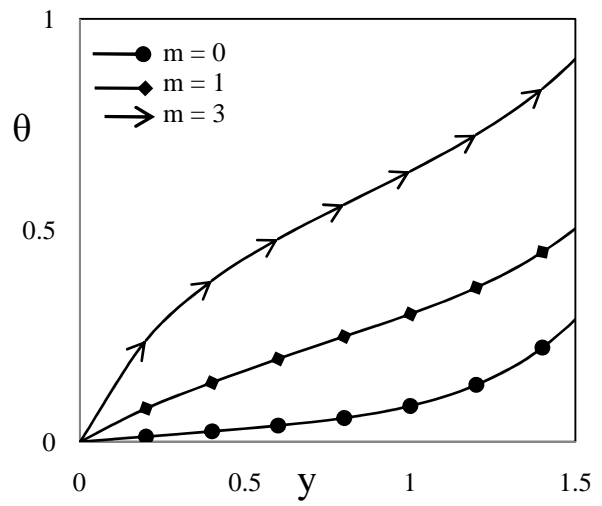
(c)  $\tau_D = 0.10$

Figure 5. Time Development of the Temperature  $\theta$  for  $S = 1$ ,  $M = 3$ ,  $m = 3$  and  $R = 2$

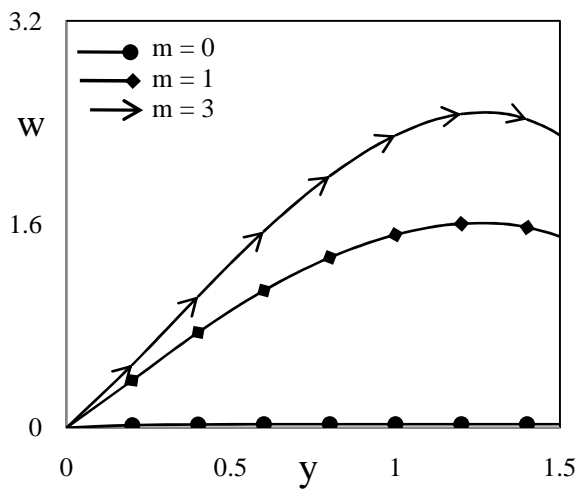
Figure 6. Effect of the Hall Parameter  $m$  on the Time Development of the Velocity Component  $u$  for  $S = 1$ ,  $M = 3$  and  $R = 2$



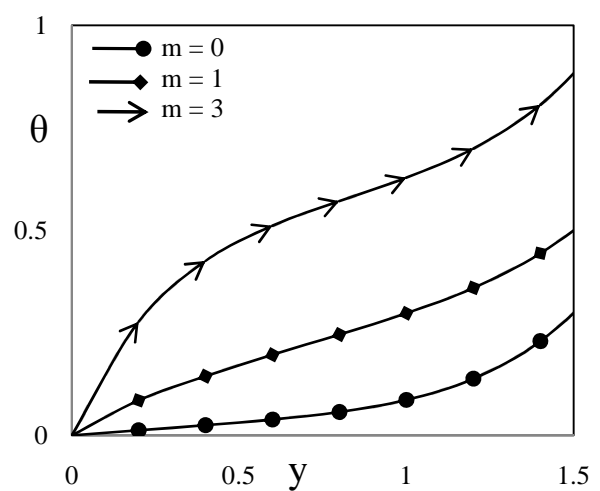
(a)  $\tau_D = 0.0$



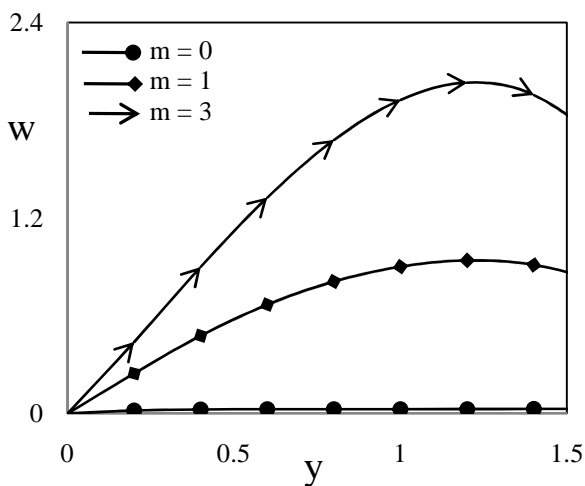
(a)  $\tau_D = 0.0$



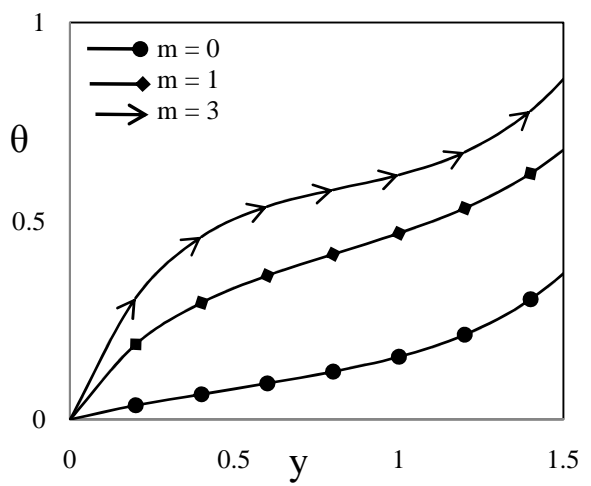
(b)  $\tau_D = 0.05$



(b)  $\tau_D = 0.05$



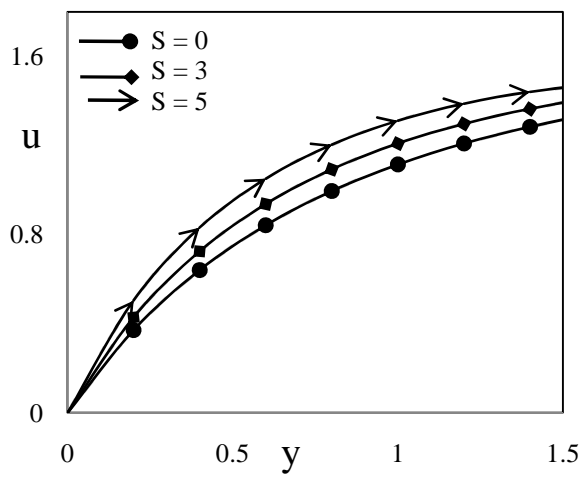
(c)  $\tau_D = 0.10$



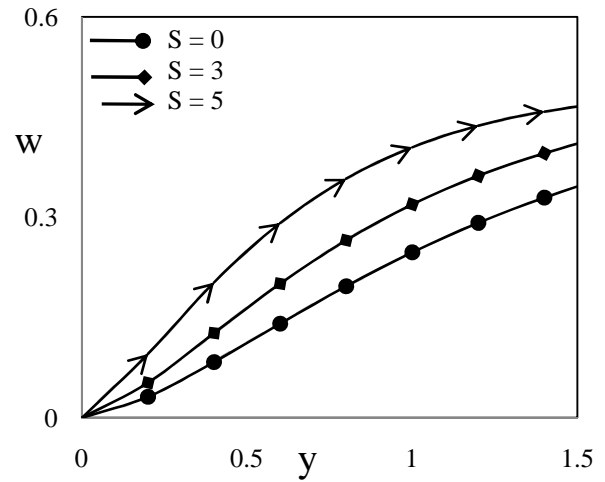
(c)  $\tau_D = 0.10$

Figure 7. Effect of the Hall Parameter  $m$  on the Time Development of the Velocity Component  $w$  for  $S = 1$ ,  $M = 3$  and  $R = 2$

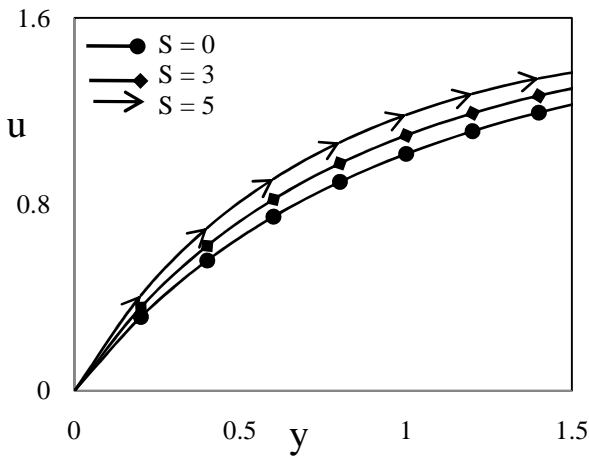
Figure 8. Effect of the Hall Parameter  $m$  on the Time Development of the Temperature  $\theta$  for  $S = 1$ ,  $M = 3$  and  $R = 2$



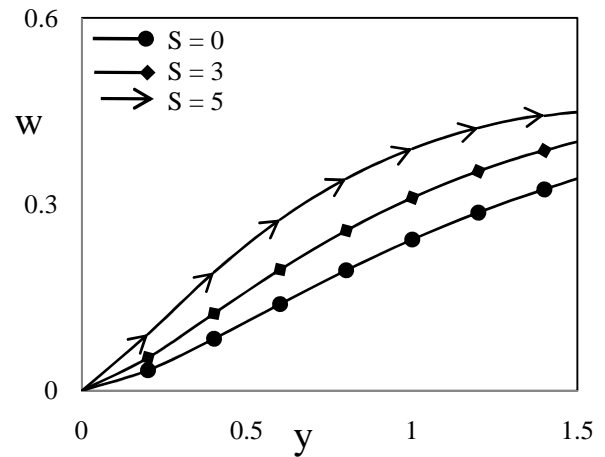
(a)  $\tau_D = 0.0$



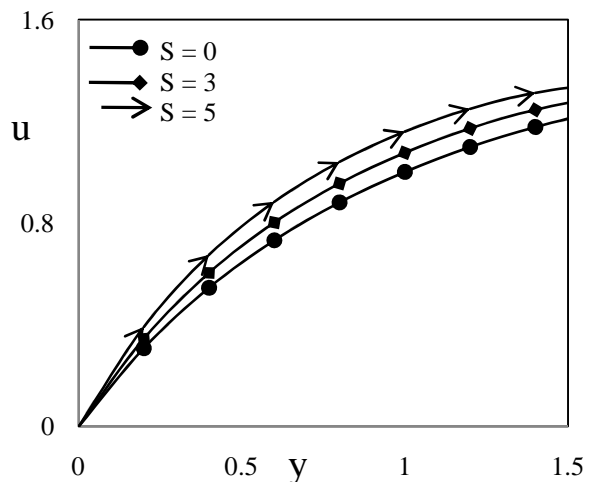
(a)  $\tau_D = 0.0$



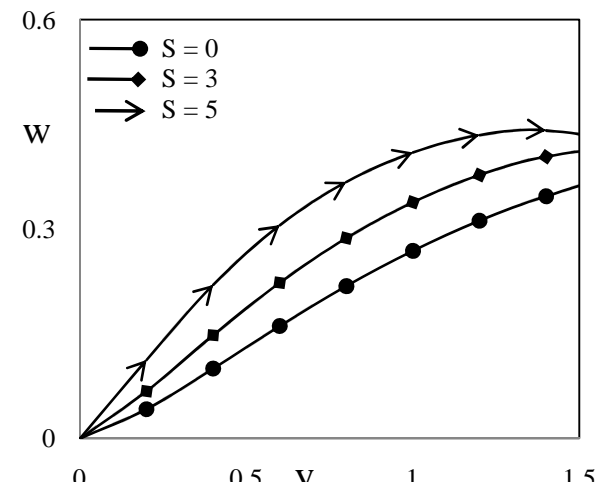
(b)  $\tau_D = 0.05$



(b)  $\tau_D = 0.05$



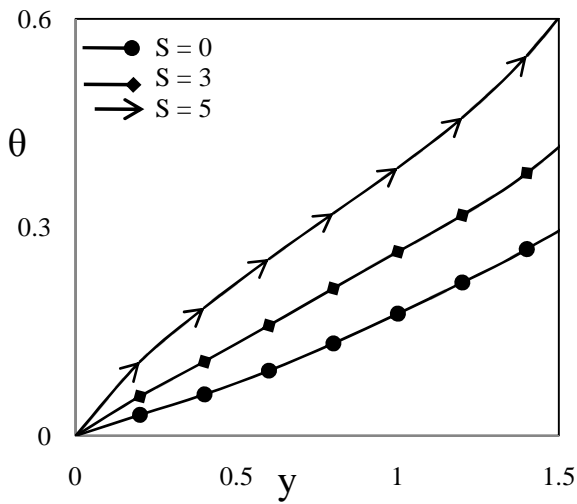
(c)  $\tau_D = 0.10$



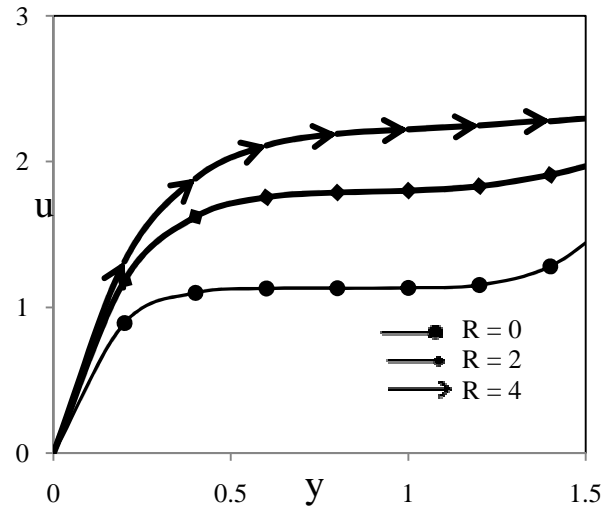
(c)  $\tau_D = 0.10$

Figure 9. Effect of the Suction Parameter  $S$  on the Time Development of the Velocity Component  $u$  for  $m = 3$ ,  $M = 3$  and  $R = 2$

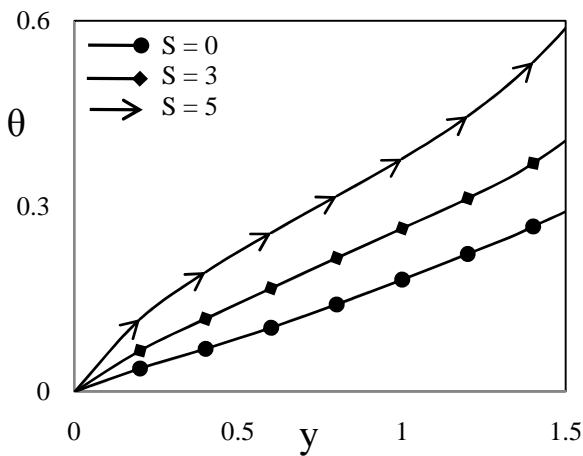
Figure 10. Effect of the Suction Parameter  $S$  on the Time Development of the Velocity Component  $w$  for  $m = 3$ ,  $M = 3$  and  $R = 2$



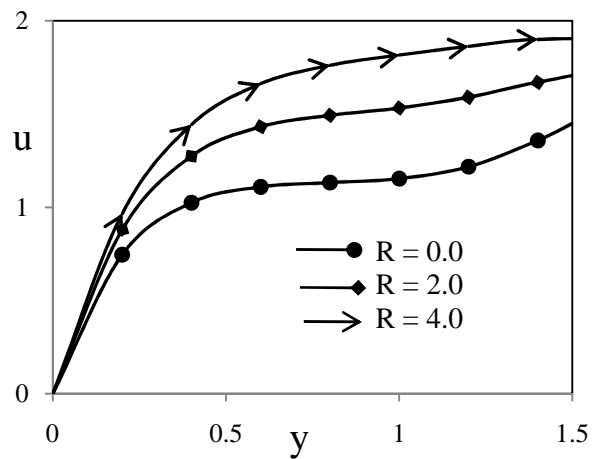
(a)  $\tau_D = 0.0$



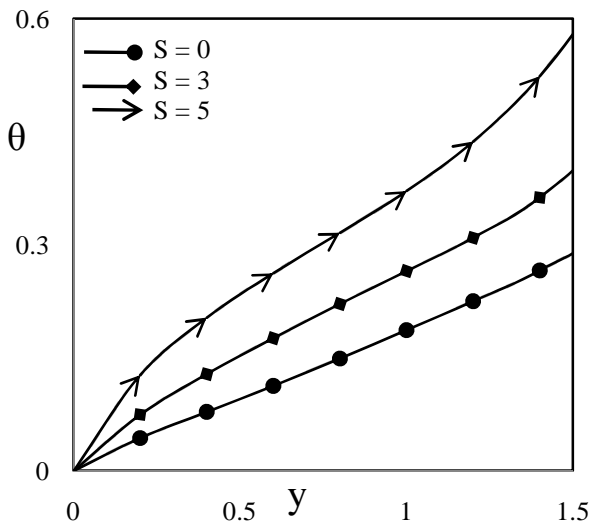
(a)  $\tau_D = 0.0$



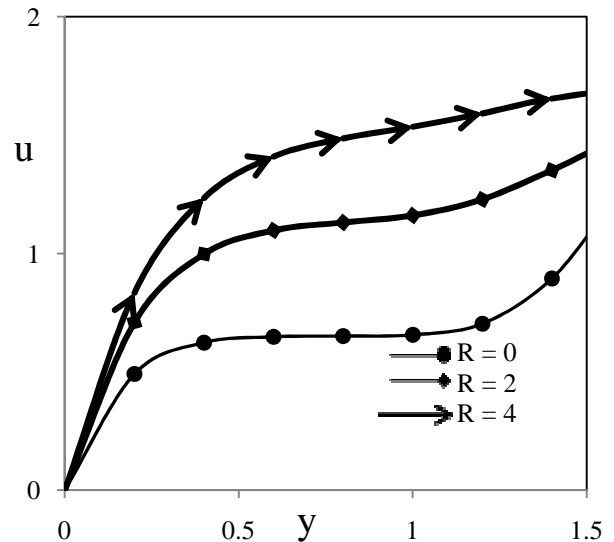
(b)  $\tau_D = 0.05$



(b)  $\tau_D = 0.05$



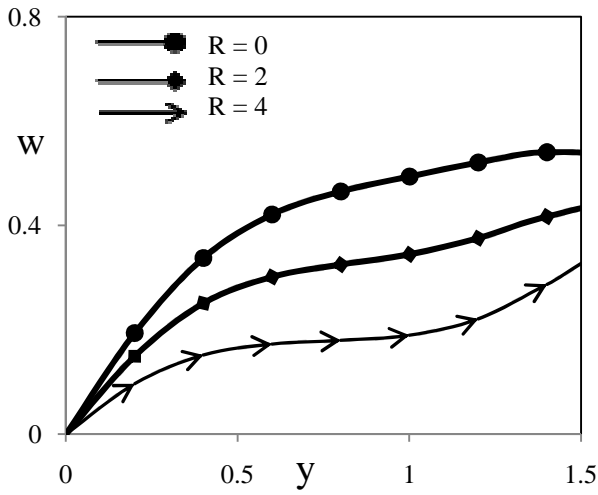
(c)  $\tau_D = 0.10$



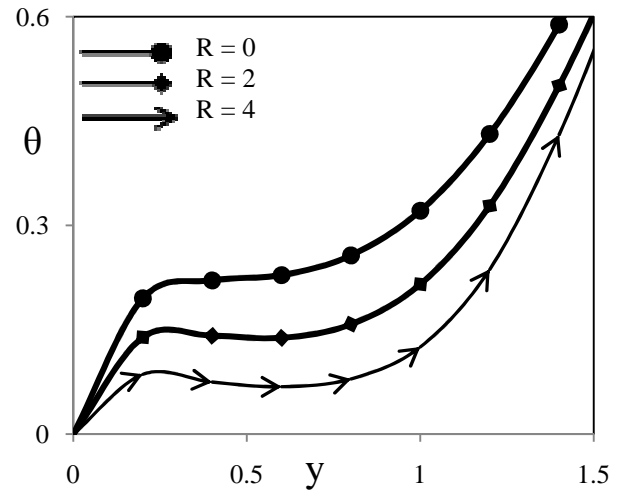
(c)  $\tau_D = 0.10$

Figure 11. Effect of the Suction Parameter  $S$  on the Time Development of the Temperature  $\theta$  for  $m=3$ ,  $M=3$  and  $R=2$

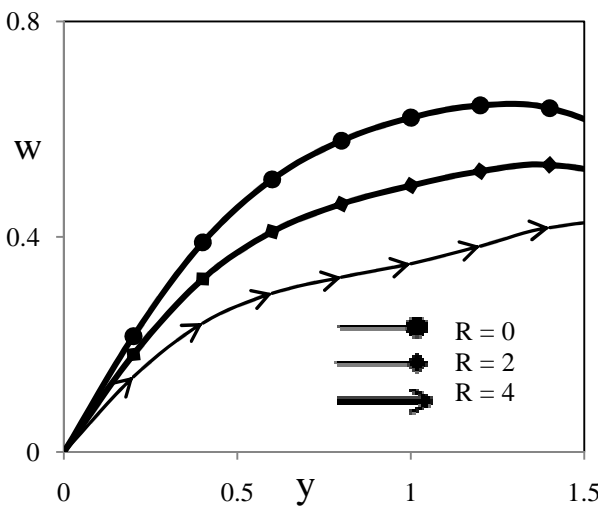
Figure 12. Effect of the Thermal Radiation Parameter  $R$  on the Time Development of the Velocity Component  $u$  for  $m=3$ ,  $M=3$  and  $S=1$



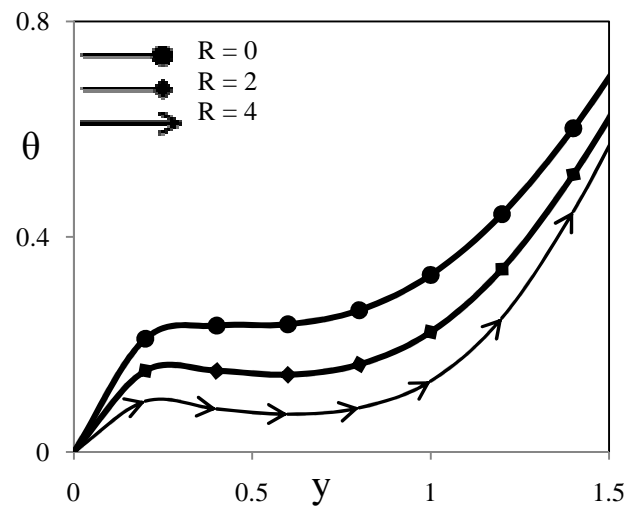
(a)  $\tau_D = 0.0$



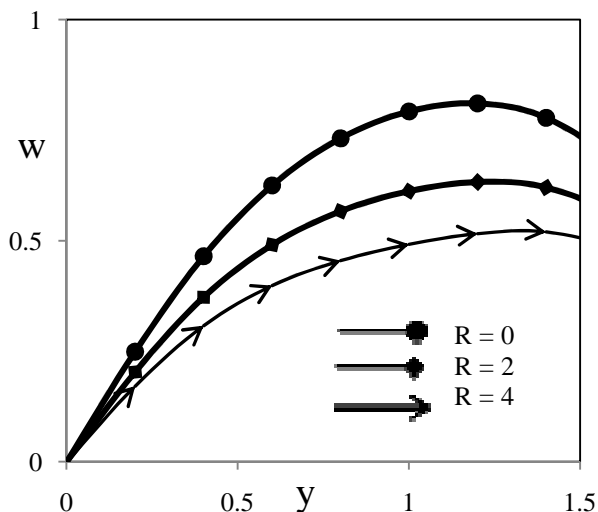
(a)  $\tau_D = 0.0$



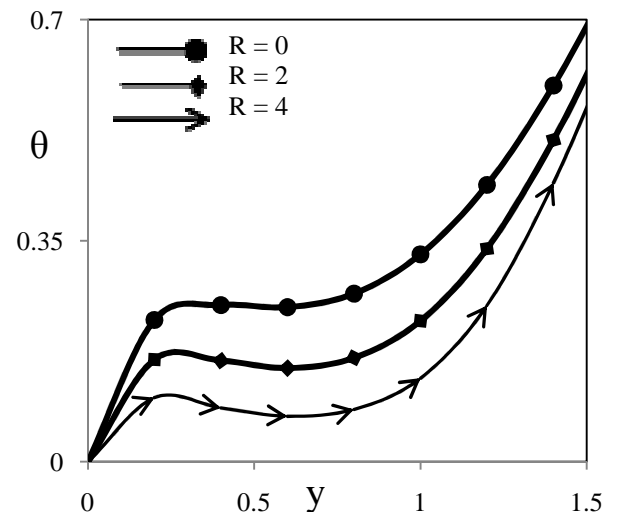
(b)  $\tau_D = 0.05$



(b)  $\tau_D = 0.05$



(c)  $\tau_D = 0.10$



(c)  $\tau_D = 0.10$

Figure 13. Effect of the Thermal Radiation Parameter  $R$  on the Time Development of Velocity Component  $w$  for  $m = 3$ ,  $M = 3$  and  $S = 1$

Figure 14. Effect of the Thermal Radiation Parameter  $R$  on the Time Development of Temperature  $\theta$  for  $m = 3$ ,  $M = 3$  and  $S = 1$

## V. CONCLUSIONS

A numerical solution to an unsteady magneto hydrodynamic the numerical solution of unsteady magneto hydrodynamic flow of an electrically conducting viscous incompressible non – Newtonian Bingham fluid bounded by two parallel non – conducting porous plates is studied with thermal radiation considering the Hall Effect have been derived. The dimensionless governing coupled, non – linear boundary layer partial differential equations are solved by an efficient, accurate, and extensively validated and unconditionally stable finite difference scheme of the Crank – Nicolson method, which is more economical from a computational point of view. The effects of the Bingham number  $\tau_D$ , the Hall parameter  $m$ , thermal radiation parameter  $R$  and the suction parameter  $S$  on the velocity and temperature distributions are studied. The Hall term affects the main velocity component  $u$  in the  $x$  – direction and gives rise to another velocity component  $w$  in the  $z$  – direction. An overshooting in the velocity components  $u$  and  $w$  with time due to the Hall Effect is observed for all values of  $\tau_D$ . The flow index  $\tau_D$  has an apparent effect in controlling the overshooting in  $u$  or  $w$  and the time at which it occurs. The results show that the influence of the parameter  $\tau_D$  on  $u$  and  $w$  depends on  $m$  and becomes more apparent when  $m$  is large. It is found also that the effect of  $m$  on  $w$  depends on  $t$  for all values of  $\tau_D$  which accounts for a crossover in the  $w$  –  $t$  graph for various values of  $m$ . The effect of  $m$  on the magnitude of  $\theta$  depends on  $n$  and becomes more pronounced in case of small  $\tau_D$ . The time at which  $u$  and  $w$  reach the steady state increases with increasing  $m$ , but decreases when  $\tau_D$  increases. The time at which  $\theta$  reaches its steady state increases with increasing  $m$  while it is not greatly affected by changing  $\tau_D$ . The effect of thermal radiation parameter  $R$  on velocity components  $u$ ,  $w$  and the temperature by changing the values of Bingham number  $\tau_D$ . As thermal radiation parameter  $R$  increases, the velocity components  $u$ ,  $w$  and temperature  $\theta$  fields are decreases with increasing values of  $\tau_D$ .

## REFERENCES

- [1] Jana, R. N. and Datta, N., (1977). Couette flow and heat transfer in a rotating system, *Acta Mechanical*, Vol. 26, pp. 301 – 306.
- [2] Singh, A. K., Sacheti, N. C. and Chandran, P., (1994). Transient Effects in Magneto hydrodynamic Couette flow with rotation: Accelerated Motion, *International Journal of Engineering Sciences*, Vol. 32, pp. 133 – 139.
- [3] Kearsley, A. J., (1994). A steady state model of Couette flow with viscous heating, *International Journal of Engineering Sciences*, Vol. 32, pp. 179 – 186.
- [4] Kumar, J., Lakshmana Rao, C. and Massoudi, M., (2003). Couette flow of granular materials, *International Journal of Non – Linear Mechanics*, Vol. 38, pp. 11 – 20.
- [5] Choi, C. K., Chung, T. J. and Kim, M. C., (2004). Buoyancy effects in plane Couette flow heated uniformly from below with constant heat flux, *International Journal of Heat and Mass Transfer*, Vol. 47, pp. 2629 – 2636.
- [6] Hashemabadi, S. H., Etemad, S. Gh. and Thibault, J., (2004). Forced convection heat transfer of couette – poiseuille flow of nonlinear viscoelastic fluids between parallel plates, *International Journal of Heat and Mass Transfer*, Vol. 47, pp. 3985 – 3991.
- [7] Attia, H. A., (2008). The effect of variable properties on the unsteady Couette flow with heat transfer considering the Hall Effect, *Communications in Nonlinear Science and Numerical Simulation*, Vol. 13, pp. 1596 – 1604.
- [8] Beg, O. A., Takhar, H. S., Zueco, J., Sajid, A. and Bhargava, R., (2008). Transient Couette Flow in a rotating non – Darcian porous medium parallel plate configuration: Network Simulation Method Solutions, *Acta Mechanica*, Vol. 200, pp. 129 – 144.
- [9] Schlichting, H. and Gersten, K., (2001). *Boundary-Layer Theory*, 8<sup>th</sup> Revised and Enlarged Edition, Springer.
- [10] Aung, W., (1972). Fully developed laminar free convection between vertical plates heated asymmetrically, *International Journal of Heat and Mass Transfer*, Vol. 15, No. 8, pp. 1577 – 1580.
- [11] Joshi, H. M., (1988). Transient effects in natural convection cooling of vertical parallel plates, *International Communications in Heat and Mass Transfer*, Vol. 15, pp. 227 – 238.
- [12] Barletta, A., (1999). Heat transfer by fully developed flow and viscous heating in a vertical channel with prescribed wall heat fluxes, *International Journal of Heat and Mass Transfer*, Vol. 42, pp. 3873 – 3885.
- [13] Jha, B. K., Singh, A. K. and Takhar, H. S., (2003). Transient free convection flow in a vertical channel due to symmetric heating, *International Journal of Applied Mechanics and Engineering*, Vol. 8, No. 3, pp. 497 – 502.
- [14] Campo, A., Manca, O. and Morrone, B., (2006). Numerical investigation of the natural convection flows for low – Prandtl fluids in vertical parallel – plates channels, *ASME Journal of Applied Mechanics*, Vol. 73, pp. 96 – 107.
- [15] Singh, A. K. and Paul, T., (2006). Transient natural convection between two vertical walls heated/cooled asymmetrically, *International Journal of Applied Mechanics and Engineering*, Vol. 11, No. 1, pp. 143 – 154.
- [16] Narahari, M., (2009). Oscillatory plate temperature effects of free convection flow of dissipative fluid between long vertical parallel plates, *International Journal of Applied Mathematics and Mechanics*, Vol. 5, No. 3, pp. 30 – 46.
- [17] Singh, A. K., (1988). Natural convection in unsteady Couette motion, *Defense Science Journal*, Vol. 38, No. 1, pp. 35 – 41.
- [18] Jha, B. K., (2001). Natural convection in unsteady MHD Couette flow, *Heat and Mass Transfer*, Vol. 37, pp. 329 – 331.
- [19] Jain, N. C. and Gupta, P., (2006). Three dimensional free convection Couette flow with transpiration cooling, *Journal of Zhejiang University Science A*, Vol. 7, No. 3, pp. 340 – 346.
- [20] Barletta, A. and Magyari, E., (2008). Buoyant Couette – Bingham flow between vertical parallel plates, *International Journal of Thermal sciences*, Vol. 47, pp. 811 – 819.
- [21] Barletta, A., Lazzari, S. and Magyari, E., (2008). Buoyant Poiseuille – Couette flow with viscous dissipation in a vertical channel, *Zeitschrift für angewandte Mathematic und Physik ZAMP*, Vol. 59, pp. 1039 – 1056.
- [22] Vradis, G. C., Dougher, J. and Kumar, S., (1993). Entrance pipe flow and heat transfer for a Bingham plastic, *Int. J. Heat Mass transfer*, Vol. 96, pp. 543–550.
- [23] Bird, R.B., Dai, G.C. and Yarusso, B.J., (1983). The rheology and flow of visco – plastic materials, *Rev. Chem. Engg.*, Vol. 1, pp. 36–69.

# The Effect of Hall Current on Unsteady MHD Free Convective Couette Flow of a Bingham Fluid with Thermal Radiation

- [24] Walton, I. C. and Bittleston, S.H., (1991). The axial flow of a Bingham plastic in a narrow eccentric annulus, *J. Fluid Mech.*, Vol. 222, pp. 39–60.
- [25] Patel, N. and Ingham, D. B., (1994). Mixed convection flow of a Bingham plastic in an eccentric annulus, *Int. J. Heat Flow*, Vol. 15, No. 2, pp. 132–141.
- [26] Min, T., Yoo, J. Y. and Choi, H., (1997). Laminar convective heat transfer of a Bingham plastic in a circular pipe. II. Numerical approach – hydro dynamically developing flow and simultaneously developing flow, *Int. J. Heat Mass Transfer*, Vol. 40, No. 15, pp. 3689–3701.
- [27] Petrov, A. G., (2000). The development of the flow of viscous and visco – plastic media between two parallel plates, *J. Appl. Math. Mech.*, Vol. 64, No. 1, pp. 123–132.
- [28] Seddeek, M. A., (2002). Effects of radiation and variable viscosity on a MHD free convection flow past a semi – infinite flat plate with an aligned magnetic field in the case of unsteady flow, *Int. J. Heat and Mass Transfer*, Vol. 45, pp. 931– 945.
- [29] Viskanta, R. and Grosh, R. J., (1962). Boundary layer in thermal radiation absorbing and emitting media, *Int. J. Heat and Mass Transfer*, Vol. 5, pp. 795–806.
- [30] Cess, R. D., (1966). The interaction of thermal radiation with free convection heat transfer, *Int. J. Heat and Mass Transfer*, Vol. 9, pp. 1269– 1277.
- [31] Sparrow, E. M. and Cess, R. D., (1966). *Radiation heat transfer*, Belmont, Calif.: Brooks/Cole.
- [32] Howell, J. R., Siegel, R. and Menguc, M. P., (2010). *Thermal radiation heat transfer*, 5th ed. FL: CRC Press.
- [33] Takhar, H. S., Gorla, R. S. R. and Soundalgekar, V. M., (1966). Short communication radiation effects on MHD free convection flow of a gas past a semi – infinite vertical plate, *Int. J. Numer. Methods Heat Fluid Flow*, Vol. 6, pp. 77–83.
- [34] Raptis, A. and Massalas, C. V., (1998). Magnetohydrodynamic flow past a plate by the presence of radiation, *Heat Mass Transfer*, Vol. 34, pp. 107– 109.
- [35] Chamkha, A. J., (2000). Thermal radiation and buoyancy effects on hydromagnetic flow over an accelerating permeable surface with heat source or sink, *Int. J. Engg. Sci.*, Vol. 38, pp. 1699– 1712.
- [36] Cookey, C. I., Ogulu, A. and Omubo – Pepple, V. B., (2003). Influence of viscous dissipation and radiation on unsteady MHD free convection flow past an infinite heated vertical plate in a porous medium with time – dependent suction, *Int. J. Heat and Mass Transfer*, Vol. 46, pp. 2305– 2311.
- [37] Ogulu, A. and Makinde, O. D., (2008). Unsteady hydromagnetic free convection flow of a dissipative and radiating fluid past a vertical plate with constant heat flux, *Chem. Engg. Commun.*, Vol. 196, pp. 454– 462.
- [38] Mahmoud, M. A. A., (2009). Thermal radiation effect on unsteady MHD free convection flow past a vertical plate with temperature dependent viscosity, *Can. J. Chem. Engg.*, Vol. 87, pp. 47 – 52.
- [39] Pop, I. and Watanabe, T., (1994). Hall effect on magnetohydrodynamic free convection about a semi – infinite vertical flat plate, *Int. J. Engg. Sci.*, Vol. 32, pp. 1903– 1911.
- [40] Abo – Eldahab, E. M. and Elbarbary, E. M. E., (2001). Hall current effect on magnetohydrodynamic freeconvection flow past a semi – infinite vertical plate with mass transfer, *Int. J. Engg. Sci.*, Vol. 39, pp. 1641– 1652.
- [41] Takhar, H. S., Roy, S. and Nath, G., (2003). Unsteady free convection flow over an infinite vertical porous plate due to the combined effects of thermal and mass diffusion, magnetic field and Hall currents, *Heat Mass Transfer*, Vol. 39, pp. 825– 834.
- [42] Saha, L. K., Siddiqua, S. and Hossain, M. A., (2011). Effect of Hall current on MHD natural convection flow from vertical permeable flat plate with uniform surface heat flux, *Appl. Math. Mech. Engl. Ed.*, Vol. 32, No. 9, pp. 1127– 1146.
- [43] Satya Narayana, P. V., Venkateswarlu, B. and Venkataramana, S., (2013). Effects of Hall current and radiation absorption on MHD micropolar fluid in a rotating system, *Ain Shams Engg. J.* <http://dx.doi.org/10.1016/j.asej.2013.02.002>.
- [44] Seth, G. S., Mahato, G. K. and Sarkar, S., (2013). Effects of Hall current and rotation on MHD natural convection flow past an impulsively moving vertical plate with ramped temperature in the presence of thermal diffusion with heat absorption, *Int. J. Energy Tech.*, Vol. 5, No. 16, pp. 1–12.
- [45] Schlichting, H., (1986). *Boundary Layer Theory*, McGraw – Hill, New York, 1986.
- [46] Sutton, G. W. and Sherman, A., (1965). *Engineering Magnetohydrodynamics*, McGraw – Hill, New York.
- [47] Attia, H. A., (1998). Hall current effects on the velocity and temperature fields of an unsteady Hartmann flow, *Can. J. Phys.*, Vol. 76, No. 9, pp. 739 – 746.
- [48] Brewster, M. Q., (1992). *Thermal radiative transfer & properties*, John Wiley & Sons.
- [49] Antia, M., (1991). *Numerical Methods for Scientists and Engineers*, Tata McGraw – Hill, New Delhi.
- [50] Attia, H. A., (1998). Hall current effects on the velocity and temperature fields of an unsteady Hartmann flow, *Can. J. Phys.*, Vol. 76, No. 9, pp. 739–746.